Food and Chemical Toxicology 132 (2019) 110675

Contents lists available at ScienceDirect

Food and Chemical Toxicology

journal homepage: www.elsevier.com/locate/foodchemtox

Myo-inositol in the protection from cadmium-induced toxicity in mice kidney: An emerging nutraceutical challenge

Giovanni Pallio[a], Antonio Micali[b,*], Salvatore Benvenga[a], Alessandro Antonelli[c], Herbert R. Marini[a], Domenico Puzzolo[b], Vincenzo Macaione[a], Vincenzo Trichilo[a], Giuseppe Santoro[b], Natasha Irrera[a], Francesco Squadrito[a], Domenica Altavilla[b], Letteria Minutoli[a]

[a] Department of Clinical and Experimental Medicine, University of Messina, 98121, Messina, Italy
[b] Department of Biomedical and Dental Sciences and Morphofunctional Imaging, University of Messina, 98121, Messina, Italy
[c] Department of Clinical and Experimental Medicine, University of Pisa, 56126, Pisa, Italy

ARTICLE INFO

Keywords:
Kidney
Cadmium
Nutraceutical
Myo-inositol
MIOX
KIM-1

ABSTRACT

Cadmium (Cd) induces functional and morphological changes in kidney. Therefore, the effects of a natural nutraceutical antioxidant, myo-inositol (MI), were evaluated in mice kidneys after Cd challenge. Twenty-eight C57 BL/6 J mice were divided into these groups: 0.9% NaCl; MI (360 mg/kg/day); $CdCl_2$ (2 mg/kg/day) plus vehicle; $CdCl_2$ (2 mg/kg/day) plus MI (360 mg/kg/day). After 14 days, kidneys were processed for structural, biochemical and morphometric evaluation. Treatment with $CdCl_2$ increased urea nitrogen and creatinine in serum and augmented tumor necrosis factor-α (TNF-α) and inducible nitric oxide synthase (iNOS) expression. Furthermore, monocyte chemoattractant protein-1 (MCP-1), kidney injury molecule-1 (KIM-1) and *myo*-inositol oxygenase (MIOX) immunoreactivity, and terminal deoxynucleotidyl transferase dUTP nick end labeling (TUNEL) positive cells number were significantly higher than control and MI groups. Glutathione (GSH) content and glutathione peroxidase (GPx) activity were reduced and structural changes were evident. The treatment with MI significantly lowered urea nitrogen and creatinine levels, TNF-α and iNOS expression, MCP-1, KIM-1 and MIOX immunoreactivity and TUNEL positive cells number, increased GSH content and GPx activity and preserved kidney morphology. A protection of MI against Cd-induced damages in mice kidney was demonstrated, suggesting a strong antioxidant role of this nutraceutical against environmental Cd harmful effects on kidney lesions.

1. Introduction

Cadmium (Cd) is a relatively rare metal, naturally present in its inorganic form. It is not biodegradable and has a biological half-life of 10–30 years, so that its environmental concentration is progressively increasing (Thévenod and Lee, 2013).

Humans are particularly exposed to Cd, either in the workplace or through the inhalation or ingestion of Cd-contaminated materials (Lee and Lim, 2011). Occupational exposure is particularly high in subjects manipulating Cd-containing pigments, plastics, glass, metal alloys and nickel-Cd batteries (Morales et al., 2006). The main sources of Cd in the general population are cigarette smoke and food. Foods as cereals, vegetables, nuts and pulses, starchy roots, potatoes, and meat products are the main source of Cd exposure for the nonsmoking population (Chunhabundit, 2016). Once absorbed, Cd is initially bound to albumin in blood plasma and transported to the liver, where it is released, thus inducing the synthesis of metallothionein (MT) (Rani et al., 2014), to which Cd is bound. The Cd-MT complex is released into the bloodstream, ultrafiltered by glomeruli, and then reabsorbed predominantly in the proximal tubules by transporters such as zinc iron proteins 8 and 14, divalent metal-ion transporter 1, and transient receptor potential vanilloid 5 and 6 (Yang and Shu, 2015). Once in the tubular cells, Cd induces toxic effects within the cells, tubular dysfunction, and lastly renal cancer (Tsutsumi et al., 2014).

Indeed, the main target of Cd is considered the kidney (Tsutsumi et al., 2014), where it accumulates, owing to the lack of an efficient mechanism for its elimination (Fouad and Jresat, 2011).

As to the mechanism of Cd renal toxicity, stimulation of

* Corresponding author. Department of Biomedical and Dental Sciences and Morphofunctional Imaging, Torre Biologica, 1st floor, University of Messina, Via C. Valeria 1, 98125, Messina, Italy.
E-mail address: amicali@unime.it (A. Micali).

https://doi.org/10.1016/j.fct.2019.110675
Received 30 April 2019; Received in revised form 21 June 2019; Accepted 11 July 2019
Available online 12 July 2019

Abbreviations

$CdCl_2$	cadmium chloride
MI	myo-inositol
ROS	Reactive Oxygen Species
GSH	glutathione
GPx	glutathione peroxidase
HE	hematoxylin and eosin
PAS	periodic acid Schiff
iNOS	inducible nitric oxide synthase
TNFα	tumor necrosis factor α
KIM-1	kidney injury molecule-1
MCP-1	monocyte chemoattractant protein-1
MIOX	*myo*-inositol oxygenase
TUNEL	terminal deoxynucleotidyl transferase dUTP nick end labeling

inflammatory pathways (Fouad and Jresat, 2011) and of cellular death by apoptosis (Gobe and Crane, 2010), injury of mitochondria (Thévenod, 2009), and disruption of cell-to-cell adhesions of the tubular cells (Prozialeck and Edwards, 2012) were described. However, an important mechanism was considered the oxidative stress, correlated to the role of Cd in replacing iron and copper from many cellular proteins, resulting in an increased concentration of these unbound ions. These latter induce oxidative stress via Fenton reactions (Rani et al., 2014). As a result, reactive oxygen species (ROS) are produced, which activate signaling molecules and proinflammatory cytokines, inducing renal tissue damage (Thévenod, 2003; Fouad and Jresat, 2011).

Therefore, many therapeutic approaches were suggested to counteract the structural and functional damages resulting from environmental or experimental Cd exposure, with particular regard to the protective functions of natural, nutraceutical antioxidants, such as curcumin (Mohajeri et al., 2017; Kim et al., 2018), betaine (Hagar and Al Malki, 2014), grape seed procyanidin (Nazima et al., 2015), alpha-lipoic acid (Luo et al., 2017), selenium (Bao et al., 2017) and, more recently, flavocoxid (Micali et al., 2018).

Among the natural nutraceutical antioxidants, myo-inositol (MI) had a significant role in reducing oxidative stress, as demonstrated by the increased levels of superoxide dismutase (SOD), catalase (CAT) and glutathione (GSH) in juvenile Jian carp (Jiang et al., 2011). In addition, an important positive role in peripheral nerves development and function (Chau et al., 2005), in osteogenesis (Dai et al., 2011), and in human reproduction (Condorelli et al., 2011, 2012; Caprio et al., 2015) was demonstrated.

Laboratory studies demonstrated that Cd adversely affects adipose tissue physiopathology through several mechanisms associated with increased production of oxidizing species or a significant decrease in the effectiveness of antioxidant defenses, thus contributing to increased insulin resistance and enhancing diabetes (Tinkov et al., 2017); intriguingly, a supplementation with a combination of MI and d-chiro-inositol is an effective and safe strategy for improving glycemic control in type 2 diabetes (Pintaudi et al., 2016). No data, however, are still available on the role of MI in the urinary apparatus, in particular in kidney.

Therefore, we performed a biochemical, morphological and morphometric study in mice challenged with Cd and administered with MI, in order to evaluate the role of this nutraceutical antioxidant in kidney and to suggest a new possible therapeutic approach of human nephrotoxicity in subjects exposed to environmental Cd.

2. Materials and methods

2.1. Experimental protocol

All procedures comply with the standards for care and use of animal subjects as stated in the ARRIVE (Animal Research: Reporting In Vivo Experiments) guidelines and with the National Institutes of Health guide for the care and use of Laboratory animals (NIH Publications No. 8023, revised 1978); the procedures were also approved by the Institutional Animal Care and Use Committee of the University Hospital of Messina, Messina, Italy. Twenty-eight male C57 BL/6 J mice (25–30 g) were purchased from Charles River Laboratories Italia srl (Calco, LC, Italy) and housed at the animal facility of the School of Medicine of the University of Messina, Messina, Italy. The animals were provided a standard diet *ad libitum* with free access to tap water and maintained on a 12-h light/dark cycle. The animals were divided into 4 groups of 7 animals each. Two groups were used as controls: 0.9% NaCl (vehicle; 1 ml/kg/day i.p.); MI (360 mg/kg/day per os). The other two groups were challenged respectively with $CdCl_2$ (2 mg/kg i.p.) plus vehicle (Minutoli et al., 2015) and $CdCl_2$ (2 mg/kg i.p.) plus MI (360 mg/kg per os) (Benvenga et al., in press). The above procedures lasted 14 days; all mice were sacrificed 24 h after the last treatment with an overdose of ketamine and xylazine and bilateral nephrectomies were performed. Each kidney was cut into two halves: one half was stored at −80 °C, the second half was immediately fixed for the morphological analysis.

2.2. Serum analysis for urea nitrogen and creatinine

Blood samples were collected, left for 60 min to clot, and centrifuged for 15 min at 6000 rpm. Urea nitrogen was measured with a colorimetric kit following the manufacturer's recommendations (Roche Diagnostics GmbH, Germany). Creatinine levels were measured using an automatic analyzer (Modular Roche Diagnostics GmbH, Germany) with an enzymatic assay method.

2.3. Determination of protein content

Total cellular proteins were extracted from kidney tissue using a lysis buffer (ratio 1:5) composed by 25 mM Tris–HCl pH 7.4, 1.0 mM ethylene glycol tetraacetic acid (EGTA), 1.0 mM ethylenediamine-tetraacetic acid (EDTA), 0.5 mM phenyl methylsulphonyl fluoride, added with protease and phosphatase inhibitors [100 mM Na3VO4, aprotinin, leupeptin, pepstatin (10 μg/ml each)]. Kidney tissue was homogenized and cell lysate was centrifuged at 13000 rpm for 15 min. The obtained supernatants were used for protein content determination using a Bio-Rad protein assay (Bio-Rad, Richmond, CA, USA).

2.4. Determination of glutathione (GSH) and glutathione peroxidase (GPx) content

GSH content was determined in the kidneys of all experimental groups according to the method of Ellman (1959), as proposed by Gong et al. (2012), while glutathione peroxidase (GPx) was determined according to Flohé and Günzler (1984), as described in detail by Manna et al. (2009).

2.5. Determination of tumor necrosis factor-α (TNF-α) and inducible nitric oxide synthase (iNOS) by western blot analysis

The supernatant obtained following processing kidney tissue was diluted with Laemmli buffer (Sigma-Aldrich Srl, Milan, Italy). Protein samples were denatured in reducing buffer (62 mM Tris pH 6.8, 10% glycerol, 2% SDS, 5% b-mercaptoethanol, 0.003% bromophenol blue) and separated by electrophoresis on SDS polyacrylamide gel (6% or 10%), approximately for 1 h. The separated proteins were transferred to a PVDF membrane in a transfer buffer [39 mM glycine, 48 mM Tris-HCl

(pH 8.3), 20% methanol] at 200 mA for 1 h. The membranes were then blocked with 5% non-fat dry milk in Tris buffer solution (TBS)-0.1% Tween-20 for 1 h at room temperature. Membranes were washed three times for 10 min each in TBS-0.1% Tween-20 and incubated with a primary antibody for TNF-α (Abcam, Cambridge, UK) and iNOS (Santa Cruz, Dallas, USA) diluted in TBS-0.1% Tween-20 overnight at 4 °C. The day after the membranes were washed three times for 10 min in TBS-0.1% Tween-20 and were incubated with a specific peroxidase-conjugated secondary antibody (KPL, USA) for 1 h at room temperature. Following other washings, the membranes were analyzed by enhanced chemiluminescence (KPL, USA). Protein signals were quantified by scanning densitometry using a bio-image analysis system (C-DiGit Blot Scanner with Image Studio 4.0 software, LI-Cor, Lincoln, Nebraska, USA) and the results were expressed as relative integrated intensity compared to controls. β-Actin (Cell Signaling Technology, Beverly, MA, USA) was used to confirm equal protein loading and blotting.

2.6. Histological evaluation

The kidneys were fixed in Bouin's solution, dehydrated in graded ethanol, cleared in xylene and embedded in paraffin (Paraplast, SPI Supplies, West Chester, PA, USA). 5 μm sections were stained with hematoxylin and eosin (HE) and periodic acid-Schiff (PAS) and photographed with a Nikon Ci-L (Nikon Instruments, Tokyo, Japan) light microscope using a digital camera Nikon Ds-Ri2.

2.7. Immunohistochemistry for monocyte chemoattractant protein-1 (MCP-1), iNOS, kidney injury molecule-1 (KIM-1) and myo-inositol oxygenase (MIOX)

From the same specimens used for histological evaluation, paraffin-embedded 5 μm sections were mounted on Polysine slides (Thermo Fisher Scientific, Waltham, MA, USA), cleared in xylene and rehydrated in decreasing concentrations of ethanol. Antigen retrieval was performed with pH 6.0 buffer citrate and endogenous peroxidase was blocked with 3.0% H_2O_2 in phosphate buffer solution (PBS). Primary antibodies (MCP-1, 1:150, Santa Cruz, Dallas, USA; iNOS, 1:100, Santa Cruz, Dallas, USA; KIM-1, 1:100, Abcam, Cambridge, UK; MIOX; 1:150; Santa Cruz, Dallas, USA) were incubated overnight at 4 °C in a moisturized chamber. The day after, secondary antibodies (anti-mouse and anti-rabbit, Vectastain, Vector, Burlingame, CA, USA) were added and the reaction was visualized with 3,3′-Diaminobenzidine (DAB) (Sigma-Aldrich, Milan, Italy). Counterstaining was performed in Mayer's hematoxylin. Negative control sections were tested using PBS instead of primary antibodies. Slides were photographed with a Nikon Ci-L (Nikon Instruments, Tokyo, Japan) light microscope using a digital camera Nikon Ds-Ri2.

2.8. Measurement of apoptosis with terminal deoxynucleotidyl transferase dUTP nick end labeling (TUNEL) assay

For the TUNEL technique, an apoptosis detection kit (In situ Apoptosis Detection kit, Abcam, Cambridge, UK) was used. From the same blocks used for histological evaluation, 5 μm sections were cleared in xylene and rehydrated in graded ethanol. After permeabilization with proteinase K, the activity of endogenous peroxidase was stopped with 3% H_2O_2 in methanol. Sections were incubated with terminal deoxynucleotidyl transferase, with biotin-labeled deoxynucleotides, with streptavidin-horseradish peroxidase conjugate, and lastly with the diaminobenzidine solution. The slides were photographed with a Nikon Ci-L (Nikon Instruments, Tokyo, Japan) light microscope using a digital camera Nikon Ds-Ri2.

2.9. Morphometric evaluation

All quantitative evaluations were performed independently by two blind investigators (DP and AM). Images of twenty glomeruli from the cortical region obtained from ten HE-stained non serial sections of each group were analyzed using the Image J software (National Institute of Health, Bethesda, MD, USA) to determine the mean total glomerular area (TGA), expressed in square micrometers (μm^2) (Yamamoto et al., 2004).

Tubular damage was evaluated from twenty microscopic fields (800 X) obtained from PAS-stained non serial sections of each group according to the following arbitrary score: 0 = normal staining with no tubular damage; 0.5 = reduced staining of the brush border with or without interstitial edema; 1 = thinning of the tubular epithelia with reduced staining of the brush border; 2 = partial absence of the tubular epithelium; 3 = tubular necrosis with or without interstitial edema (Kiss et al., 2003; Okada et al., 2015).

A morphometric study to quantitatively assess MCP-1, iNOS, KIM-1 and MIOX expression was also carried out using the public domain ImageJ software. The RGB color images were converted in 32-bit grayscale images, using the function Image > type > 32-bit. A unit area (UA) of 200 × 200 μm, including only tubules, was selected and the grayscale values (function: analyze > measure) of twenty UAs of each group were calculated in optical units (OU) from 0 = black to 255 = white. In this way, a higher expression of MCP-1, iNOS, KIM-1 and MIOX corresponded to darker images and was reported as lower values in the 0–255 grayscale; a lower expression of MCP-1, iNOS, KIM-1 and MIOX was indicated by lighter images, corresponding to higher values on the same scale. The distribution of apoptosis in the proximal tubules from each group, expressed as apoptotic index (AI), was obtained by dividing the number of TUNEL-positive tubular cells by the total number of tubular cells in twenty microscopic fields and the result was multiplied by 100.

2.10. Drugs and chemicals

$CdCl_2$ was purchased from Sigma-Aldrich Srl (Milan, Italy). MI was a kind gift of LO.LI. Pharma S.r.l. (Rome, Italy). All other chemicals not otherwise mentioned were commercially available reagent grade. $CdCl_2$ was dissolved every day in 0.9% NaCl, while MI was ready for use.

2.11. Statistical analysis

The statistical significance of differences among groups was performed with ANOVA comparison test, followed by the Bonferroni post hoc test. The MedCalc 12.2.1.0 statistical software (MedCalc Software, Ostend, Belgium) was used. Values were provided as mean ± standard deviation (SD). A p value of ≤ 0.05 was considered statistically significant.

3. Results

3.1. MI effects on urea nitrogen and creatinine

No significant differences in urea nitrogen and creatinine levels were observed in the serum of control and MI alone groups. In mice challenged with $CdCl_2$, urea nitrogen and creatinine levels were significantly increased when compared to control group. In $CdCl_2$ challenged animals co-treated with MI, a significant difference versus $CdCl_2$ alone treated mice was demonstrated, being urea nitrogen and creatinine levels similar to control mice (Table 1).

3.2. MI effects on GSH and GPx content

No significant differences in GSH content and GPx activity were observed in control and MI alone groups. A significant decrease in GSH content and in GPx activity was observed in Cd-challenged mice. When $CdCl_2$ challenged animals were treated with MI, both GSH and GPx showed significantly higher values versus $CdCl_2$ alone, being similar to

Table 1
Urea nitrogen and creatinine levels in control mice, in myo-inositol (MI) (360 mg/kg/day) alone treated mice, in cadmium chloride ($CdCl_2$; 2 mg/kg i.p.) plus vehicle exposed mice and in mice exposed to $CdCl_2$ (2 mg/kg i.p.) coadministered with MI.

	Urea nitrogen (mg/dl)	Creatinine (mg/dl)
Control (0.9% NaCl)	13.9 ± 1.4	0.61 ± 0.08
MI (360 mg/kg/day)	14.1 ± 1.6	0.64 ± 0.12
$CdCl_2$ + vehicle	39.3 ± 4.4[a]	1.48 ± 0.28[a]
$CdCl_2$ + MI	15.5 ± 1.2[b]	0.69 ± 0.11[b]

All the values are expressed as mean ± SD, n = 7 animals for each group.
[a] $p < 0.05$ vs controls.
[b] $p < 0.05$ vs $CdCl_2$ + vehicle.

control mice (Table 2).

3.3. MI effects on TNFα and iNOS expression

No significant difference in TNFα expression was observed in control and MI alone groups. $CdCl_2$ administration induced a five folds increase of TNFα expression. In mice treated with $CdCl_2$ and co-administered with MI, TNFα expression was similar to controls (Fig. 1 A).

When iNOS was taken into account, $CdCl_2$ challenge induced a significant increase of its expression. On the contrary, in $CdCl_2$ challenged animals co-treated with MI iNOS expression was similar to control mice (Fig. 1 B).

3.4. Histological and morphometric evaluation

For histological evaluation, kidney sections stained with HE and PAS were examined. In kidney sections stained with HE of control and MI alone groups, glomeruli and tubules showed normal histological organization (Fig. 2 A, B). In $CdCl_2$ challenged mice, glomeruli with enlarged Bowman's space, proximal tubules with epithelial damages and an interstitial edema were observed (Fig. 2 C). In $CdCl_2$ challenged mice administered with MI, cellular lesions and interstitial edema were absent, with normal glomerular and tubular morphology (Fig. 2 D). The morphometric evaluation of the glomerular area demonstrated a significant higher surface in $CdCl_2$ challenged mice, when compared to control and MI alone groups. In $CdCl_2$ challenged mice administered with MI glomerular area was similar to control groups (Fig. 2 E).

When kidney sections were stained with PAS, proximal tubules of control and MI alone groups showed a regular and well stained brush border (Fig. 3 A, B). On the contrary, in $CdCl_2$ challenged mice, the brush border was particularly thin or absent and tubular epithelial lesions and interstitial edema were also present (Fig. 3 C). In $CdCl_2$ challenged mice administered with MI, tubules showed PAS-positive brush border and had normal organization (Fig. 3 D). The morphometric evaluation of the tubular damage demonstrated a higher score in $CdCl_2$ challenged mice and a significant reduction, similar to control and MI alone groups, in $CdCl_2$ plus MI treated mice (Fig. 3 E).

3.5. Immunohistochemistry for MCP-1, iNOS, KIM-1 and MIOX

In control and MI alone groups, MCP-1 immunoreactivity was undetectable (Fig. 4 A, B). In $CdCl_2$ plus vehicle treated mice, nearly all tubules showed a strong MCP-1 immunoreactivity (Fig. 4 C). In mice treated with $CdCl_2$ plus MI, MCP-1 immunoreactivity was similar to control and MI alone groups (Fig. 4 D). The quantitative assessment of MCP-1 expression revealed significant lower values in the 0–255 grayscale in $CdCl_2$ treated mice versus controls; on the contrary, in $CdCl_2$ plus MI group, values were similar to controls (Fig. 4 E).

In control and MI alone groups, iNOS immunoreactivity was absent (Fig. 5 A, B). In $CdCl_2$ plus vehicle treated mice, iNOS immunoreactivity was particularly strong in the tubules (Fig. 5 C). In $CdCl_2$ plus MI treated mice, iNOS immunoreactivity was similar to controls (Fig. 5 D).

In control and MI alone groups, KIM-1 immunoreactivity was absent (Fig. 5E and F). In $CdCl_2$ plus vehicle treated mice, a strong KIM-1 immunoreactivity was present in the tubular cells (Fig. 5 G). In $CdCl_2$ plus MI treated mice, no KIM-1 positive cells were observed (Fig. 5 H).

The quantitative assessment of both iNOS and KIM-1 tubular expression demonstrated significant lower values in the 0–255 grayscale in $CdCl_2$ challenged mice versus controls and higher values, similar to controls, in $CdCl_2$ plus MI group (Fig. 5 I).

In control and MI alone groups, MIOX immunoreactivity was very low in the proximal tubules (Fig. 6A and B). In $CdCl_2$ plus vehicle treated mice, all proximal tubules showed an evident and diffuse MIOX immunoreactivity (Fig. 6 C). In the kidneys of $CdCl_2$ plus MI treated mice, MIOX immunoreactivity was negligible and similar to controls (Fig. 6 D). The quantitative assessment of MIOX tubular expression revealed significant lower values in the 0–255 grayscale in $CdCl_2$ treated mice versus controls, and higher values, similar to controls, in $CdCl_2$ plus MI group (Fig. 6 E).

3.6. Measurement of apoptosis with TUNEL assay

In control and MI alone groups, TUNEL positive cells were rarely detected (Fig. 7A and B). In $CdCl_2$ plus vehicle treated mice, many TUNEL-positive cells were present in the tubules (Fig. 7 C). In the tubular epithelium of $CdCl_2$ plus MI, the number of TUNEL-positive cells was dramatically reduced and similar to controls (Fig. 7 D). These data were confirmed also by the evaluation of the AI in the tubular cells (Fig. 7 E).

4. Discussion

Heavy metal-induced diseases are important public health problems, as human exposure can occur from both environmental and occupational sources (Wise et al., 2017). Among the well-known environmental toxicants, Cd has severe negative effects on the human body, and particularly on the kidney, which is considered the main target of this pollutant (Luo et al., 2017).

In biological systems, Cd is unable to perform redox reactions (Rani et al., 2014), but it can induce oxidative stress both in vivo and in vitro by depleting GSH levels (Gong et al., 2012) or by inhibiting antioxidant enzymes, such as GPx, interacting with their thiol groups (Koedrith and Seo, 2011). In our study, we confirmed that in Cd-challenged mice GSH and GPx levels were highly reduced in kidney tissue and that serum urea nitrogen and creatinine were elevated, thus indicating an important kidney involvement.

Because of renal Cd challenge, ROS are produced which trigger proinflammatory cytokines and signaling molecules production, inducing renal tissue damage (Thévenod, 2003; Fouad and Jresat, 2011).

Among the proinflammatory cytokines, TNF-α plays an important role as it is significantly elevated in chronic renal failure patients, and in rats with cisplatin- and paraquat-induced acute kidney injury (AKI)

Table 2
Glutathione (GSH) content and glutathione peroxidase (GPx) activity in control mice, in myo-inositol (MI) (360 mg/kg/day) alone treated mice, in cadmium chloride ($CdCl_2$; 2 mg/kg i.p.) plus vehicle exposed mice and in mice exposed to $CdCl_2$ (2 mg/kg i.p.) coadministered with MI.

	GSH (μmol/g tissue)	GPx (nmol/min per mg protein)
Control (0.9% NaCl)	65 ± 4	34.61 ± 1.96
MI (360 mg/kg/day)	62 ± 5	31.63 ± 1.47
$CdCl_2$ + vehicle	47 ± 5[a]	16.35 ± 0.58[a]
$CdCl_2$ + MI	64 ± 3[b]	31.22 ± 1.34[b]

All the values are expressed as mean ± SD, n = 7 animals for each group.
[a] $p < 0.05$ vs controls.
[b] $p < 0.05$ vs $CdCl_2$ + vehicle.

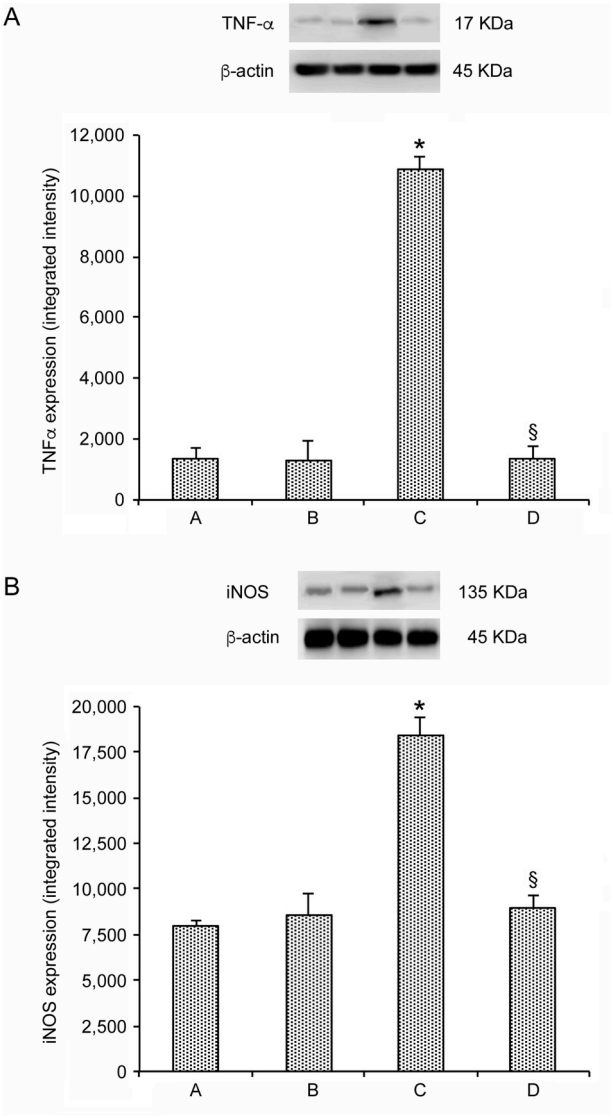

Fig. 1. Representative Western Blot analysis of TNFα (Panel A) and iNOS (Panel B) in the kidneys of control (A), MI alone (B), $CdCl_2$ plus vehicle (C), $CdCl_2$ plus MI (D) mice groups. *p < 0.05 versus control; §p < 0.05 versus $CdCl_2$ plus vehicle. Bars represent the mean ± SD of seven animals.

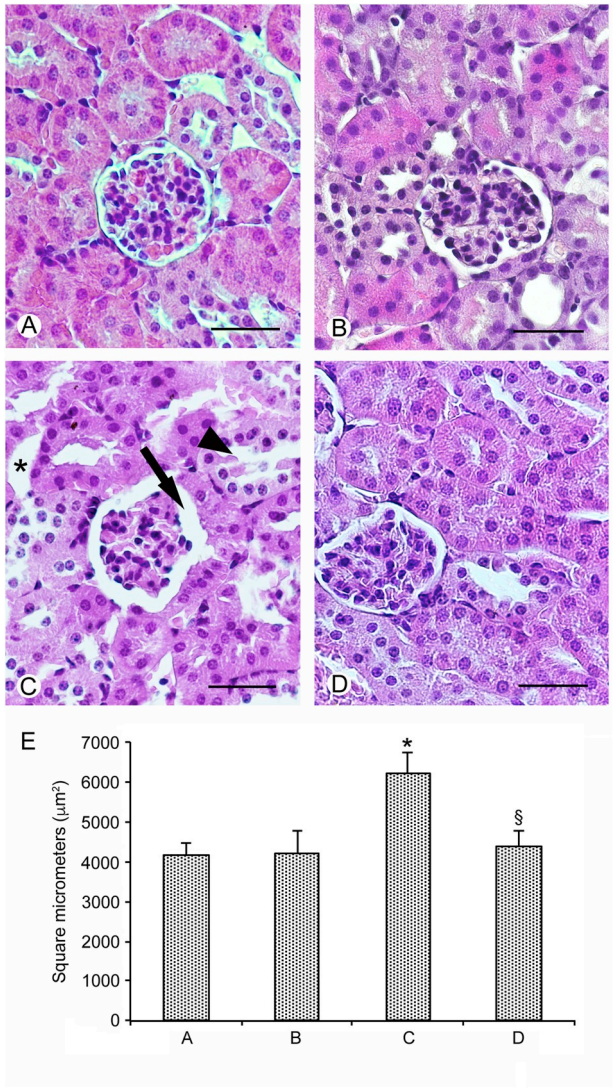

Fig. 2. Structural analysis of the kidneys of control (A), MI alone (B), $CdCl_2$ plus vehicle (C), $CdCl_2$ plus MI (D) mice. (Hematoxylin and eosin stain). A, B: In control and MI alone groups, glomeruli and tubules show normal morphology. C: In $CdCl_2$ challenged mice, glomeruli have widened Bowman's space (arrow); tubular cells show evident lesions (arrowhead). An interstitial edema is also present (*). D: In $CdCl_2$ challenged mice administered with MI, glomerular and tubular morphology is normal. E: Glomerular area expressed in μm^2. *p < 0.05 versus control; §p < 0.05 versus $CdCl_2$ plus vehicle. Bars represent the mean ± SD of seven animals. (Scale bar: 50 μm).

(Ramesh and Reeves, 2002; Gu et al., 2016; Li et al., 2018). Also in Cd-challenged mice, we demonstrated kidney TNF-α elevation, thus confirming the role of this heavy metal in promoting inflammatory pathways. TNF-α was also reported to activate apoptosis via the death receptor pathway (Yang et al., 2007). In our study, TUNEL staining revealed that apoptotic cells in the renal tubules of Cd-challenged mice were markedly increased.

Furthermore, Cd induces iNOS, responsible for nitrosative stress. iNOS is not present in normal kidney (Förstermann and Sessa, 2012) and, when produced in large amount, exerts nephrotoxic injury, with proximal tubules and glomeruli dysfunction in some experimental models, such as renal ischemia/reperfusion (Chatterjee, 2007). We examined the expression of iNOS after Cd challenge and showed its increased expression, thus corroborating its harmful role in the proximal tubules. These biochemical and molecular data were confirmed by the histopathological exam, which demonstrated an increased glomerular area, a reduced PAS stain of the proximal tubules brush border, the presence of tubular cells lesions and of interstitial edema, as already demonstrated in previous observations (Moulis and Thévenod, 2010; Rafati et al., 2015; Micali et al., 2018).

In addition to the morphological damage, Cd administration induced a marked increase of KIM-1 immunoreactivity of proximal tubules (Prozialeck et al., 2007). KIM-1 is a type 1 cell membrane glycoprotein (Ichimura et al., 2008), not detectable in normal kidney (Förstermann and Sessa, 2012), but present after an ischemic or toxic injury of the renal proximal tubule (Andreucci et al., 2017). Therefore, KIM-1 seems an ideal biomarker of kidney injury. KIM-1 was also demonstrated with immunohistochemistry in the kidneys of rats chronically challenged with Cd (Prozialeck et al., 2009) and in cats with natural and experimentally induced AKI (Bland et al., 2017). After Cd administration, we demonstrated an evident positivity for KIM-1 in the tubular epithelium.

As Cd triggers several mechanisms including inflammation (Min et al., 2002; Akinyemi et al., 2018), responsible of the initiation and progression of kidney tubulointerstitial diseases (Wang et al., 2010), we evaluated the expression of MCP-1, a potent chemokine mostly produced by tubular cells following renal injury and involved in interstitial

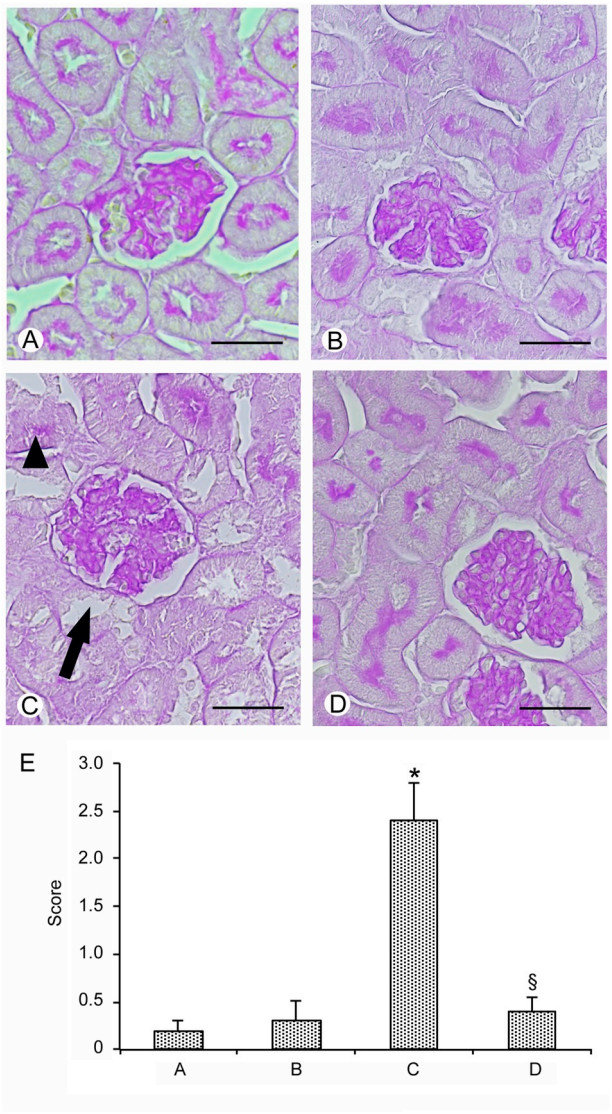

Fig. 3. Tubular brush border in the kidneys of control (A), MI alone (B), $CdCl_2$ plus vehicle (C), $CdCl_2$ plus MI (D) mice groups. (Periodic Acid Schiff stain). A, B: In control and MI alone groups the proximal tubules show a regular and well-stained brush border. C: In $CdCl_2$ challenged mice, the brush border is particularly thin or absent (arrowhead) and the tubular epithelium shows structural changes (arrow). D: In $CdCl_2$ challenged mice administered with MI, the brush border and the tubules have normal organization. E: Tubular damage score based on the brush border behavior. *p < 0.05 versus control; §p < 0.05 versus $CdCl_2$ plus vehicle. Bars represent the mean ± SD of seven animals. (Scale bar: 50 μm).

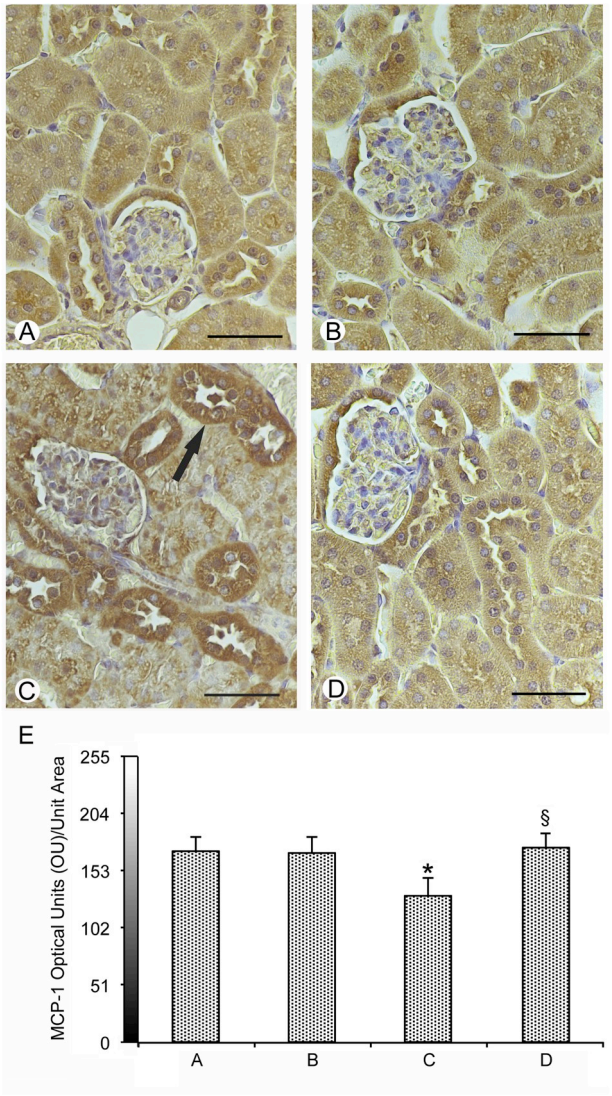

Fig. 4. Immunohistochemical localization of MCP-1 in the kidneys of control (A), MI alone (B), $CdCl_2$ plus vehicle (C), $CdCl_2$ plus MI (D) mice groups. A, B: In control and MI alone groups, no MCP-1 immunoreactivity can be demonstrated. C: In $CdCl_2$ plus vehicle-treated mice, MCP-1 immunoreactivity is particularly strong in the tubular cells (arrow). D: In $CdCl_2$ plus MI treated mice, MCP-1 immunoreactivity is absent. E: Morphometric results for MCP-1 expression. Data are expressed in Optical Units/Unit Area (OU/UA) (from 0 = black to 255 = white). *p < 0.05 versus control; §p < 0.05 versus $CdCl_2$ plus vehicle. Bars represent the mean ± SD of seven animals. (Scale bar: 50 μm).

inflammation (Wang et al., 2010). In our study, MCP-1 immunoreactivity was significantly increased in the kidneys of Cd-challenged group, particularly evident in tubules with marked cellular damages.

The effects of many protective agents in preserving against Cd-induced nephrotoxicity were studied in the last years, with particular regard to natural nutraceutical antioxidants, such as curcumin (Mohajeri et al., 2017; Kim et al., 2018), betaine (Hagar and Al Malki, 2014), grape seed procyanidin (Nazima et al., 2015), alpha-lipoic acid (Luo et al., 2017), selenium (Bao et al., 2017) and, more recently, flavocoxid (Micali et al., 2018).

As no data are currently available, we evaluated the possible role of MI, a natural nutraceutical antioxidant in this model of Cd challenge. No morphological and biochemical differences with control group were observed for all considered parameters in mice treated with MI alone. Positive tasks of MI have been demonstrated in peripheral nerves (Chau et al., 2005), in bone (Dai et al., 2011), and in human genital apparatus (Condorelli et al., 2011, 2012; Caprio et al., 2015), but no data are available on its role in the urinary apparatus, particularly in kidney. The nutraceutical efficacy of MI could be related to a direct antioxidant role, as it was able to increase GSH and GPx activity in animals challenged with copper, a heavy metal able to induce the overproduction of ROS (Jiang et al., 2011).

Moreover, it has been recently suggested that Cd can result in endoplasmic reticulum stress and oxidative stress in the kidneys of rats, activate Nrf2 signaling pathway-related factors, and upregulate the transcriptional expression of phase II detoxification enzymes under these experimental conditions (Chen et al., 2019). In addition, both in vitro and in vivo studies have shown that downstream phase II detoxification enzymes are regulated by Nrf2, and activated Nrf2 can upregulate the transcriptional expression of phase II detoxification enzymes

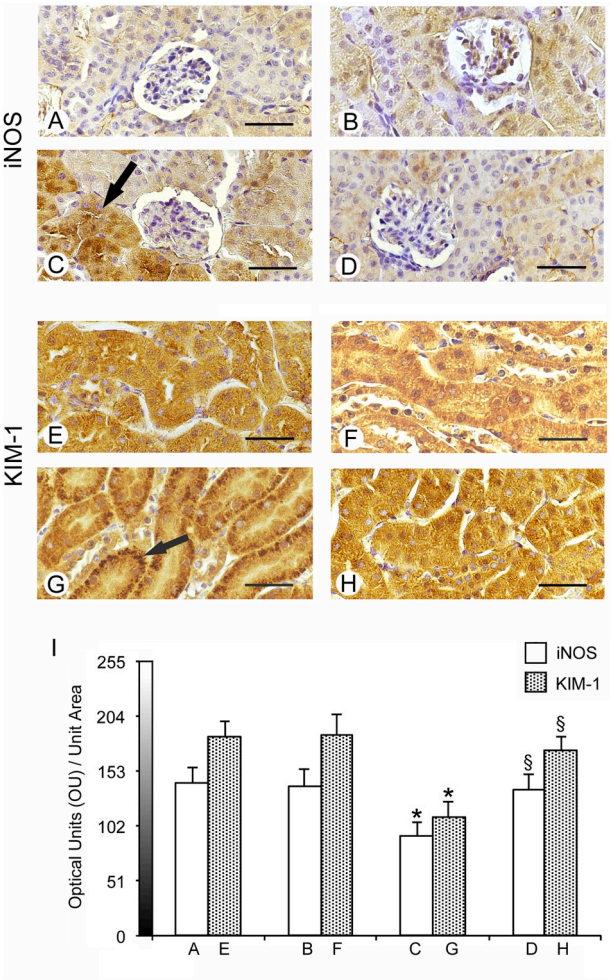

Fig. 5. Immunohistochemical localization of iNOS and KIM-1 in the kidneys of control (A), MI alone (B), $CdCl_2$ plus vehicle (C), $CdCl_2$ plus MI (D) mice groups. A, B: In control and MI alone groups, iNOS immunoreactivity is absent. C: In $CdCl_2$ plus vehicle-treated mice, iNOS immunoreactivity is particularly strong in the tubular wall (arrow). D: In $CdCl_2$ plus MI treated mice, iNOS positivity is absent. E, F: In control and MI alone groups, KIM-1 immunoreactivity is absent. G: In $CdCl_2$ plus MI treated mice, no KIM-1 positive cells are observed. I: Morphometric results for iNOS and KIM-1 expression. Data are expressed in Optical Units/Unit Area (OU/UA) (from 0 = black to 255 = white). *p < 0.05 versus control; §p < 0.05 versus $CdCl_2$ plus vehicle. Bars represent the mean ± SD of seven animals. (Scale bar: 50 μm).

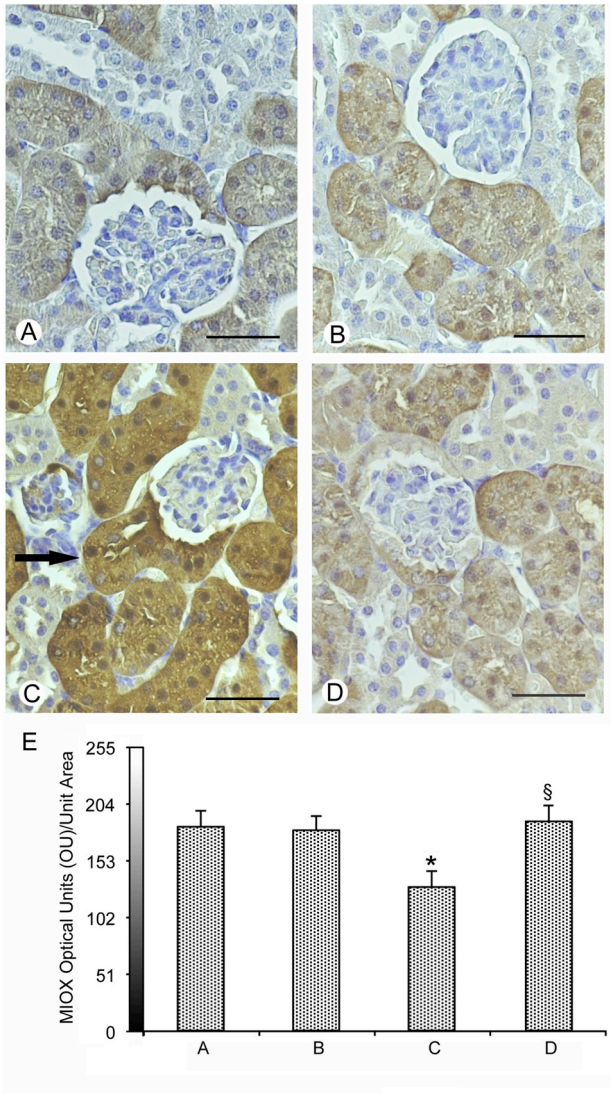

Fig. 6. Immunohistochemical localization of MIOX in the kidneys of control (A), MI alone (B), $CdCl_2$ plus vehicle (C), $CdCl_2$ plus MI (D) mice groups. A, B: In control and MI alone groups, very low MIOX immunoreactivity can be demonstrated in the proximal tubules. C: In $CdCl_2$ plus vehicle-treated mice, MIOX immunoreactivity is particularly strong in the tubular cells (arrow). D: In $CdCl_2$ plus MI treated mice, very low MIOX immunoreactivity is present. E: Morphometric results for MIOX expression. Data are expressed in Optical Units/Unit Area (OU/UA) (from 0 = black to 255 = white). *p < 0.05 versus control; §p < 0.05 versus $CdCl_2$ plus vehicle. Bars represent the mean ± SD of seven animals. (Scale bar: 50 μm).

such as GST-P1, GCLC, HO-1, and NQO1 (Liu et al., 2014; Park et al., 2015; Li et al., 2017). Interestingly, dietary MI deficiency decreased the growth performances and impaired intestinal physical barrier function partly relating to Nrf2, JNK, E2F4 and MLCK signaling in animal model, thereby responding to oxidative stress and suggesting the potential modulating antioxidant/anti-inflammatory role of nutraceutical antioxidants including MI (Li et al., 2017).

MI supplementation could also reverse the depletion of cellular content of inositol (and of its isomers and phosphate derivatives), observed in all conditions strongly characterized by oxidative stress that are mechanistically and epidemiologically associated with high-glucose diet or altered glucose metabolism (Nayak et al., 2011; Muscogiuri et al., 2016). Specifically, in course of diabetic nephropathy, the oxidative stress promotes the upregulation of the kidney specific protein MIOX (Sun et al., 2016), which catabolizes MI into D-glucuronic acid exclusively in the kidney, being confined to the proximal tubular cells (Gao et al., 2018). We demonstrated, as far as we know for the first time, that Cd challenge induced an overexpression of MIOX and that MI supplementation determined a significant reduction of MIOX expression, as assessed by immunohistochemistry. Therefore, MI at the dosage used was able to obtain significant positive effects on both biochemical and morphological parameters. As a matter of fact, in $CdCl_2$ challenged mice administered with MI, we confirmed that this nutraceutical compound impacts different molecular pathways oxidative stress related. Specifically, data of our experiments highlight the potential beneficial effect of MI supplementation on the well-known effects of Cd on the kidney.

Overall, since it has been previously emphasized that MI could have a crucial role in cellular morphogenesis and cytogenesis (i.e. *(i)* synthesis of lipids, *ii)* creation of cell membranes and *iii)* cell growth), our experimental observations could indicate that it may play a relevant nutraceutical role against Cd toxicity.

Indeed, we can also translate our research evidence in clinical practice. In fact, many studies indicate that the largest amount of MI is

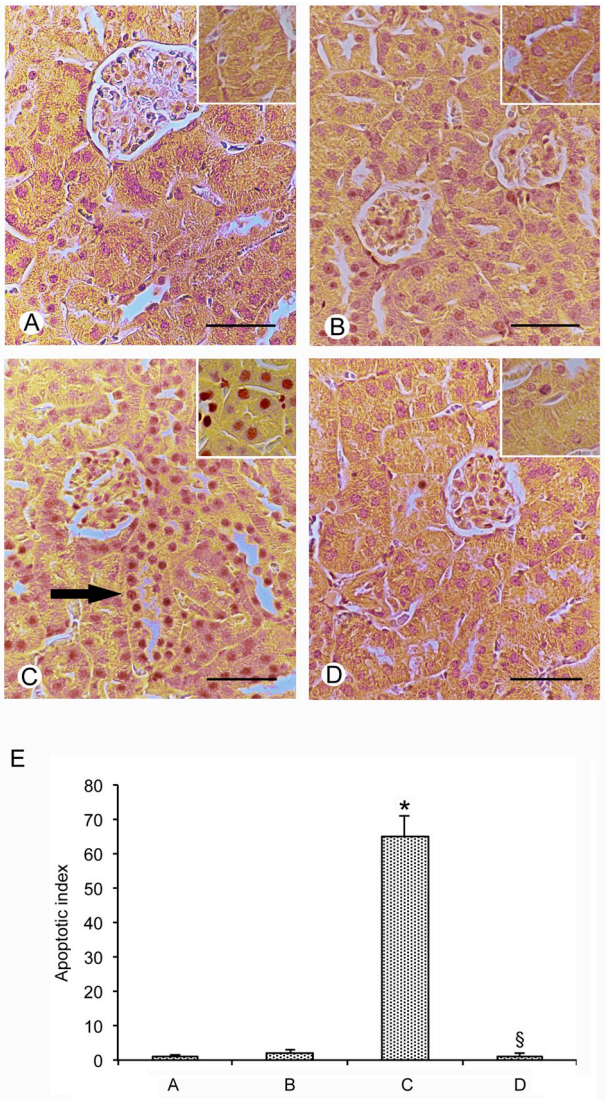

Fig. 7. Assessment of apoptosis with TUNEL staining technique in the kidneys of control (A), MI alone (B), $CdCl_2$ plus vehicle (C), $CdCl_2$ plus MI (D) mice groups. A, B: In control and MI alone groups, no TUNEL-positive cells can be observed. C: In $CdCl_2$ plus vehicle-treated mice, TUNEL-positive tubular cells (arrow) are present. D: In $CdCl_2$ plus MI treated mice, TUNEL-positive cells number is similar to controls. E: Apoptotic index of the different groups of challenged mice. *p < 0.05 versus control; §p < 0.05 versus $CdCl_2$ plus vehicle. Bars represent the mean ± SD of seven animals. (Scale bar: 50 μm).

found in foods typical of Mediterranean-style eating pattern as fresh fruits, beans, vegetables, grains and nuts (Dinicola et al., 2017). Consequently, the consumption of MI, a natural antioxidant present in large amounts in several foods, can be considered a new reliable nutraceutical strategy in humans exposed to heavy metals, at least to those provided of mechanisms of action superimposable to Cd.

Of course, both short- and long-duration epidemiological studies are required to determine the optimal doses of MI, to provide safe and effective therapeutic strategies against Cd toxicity.

5. Conclusions

In light of these results, we feel that MI might offer a new possible nutraceutical challenge that, properly combined with good agricultural practice to minimize Cd contamination in food crops and animals, could also provide a definite strategy to prevent and counteract Cd-induced kidney lesions.

Funding

This research did not receive any specific grant from funding agencies in the public, commercial, or not-for-profit sectors.

Declaration of interests

All the authors declare that they have no known competing financial interests or personal relationships that could have appeared to influence the work reported in this paper.

Conflicts of interest

The authors declare no actual or potential competing financial interests.

Acknowledgements

The work was granted by a Departmental funding. The authors thank LO.LI. Pharma S.r.l. (Rome, Italy) for the kind gift of MI and Mr. Sebastiano Brunetto from the Department of Biomedical and Dental Sciences and Morphofunctional Images of the University of Messina for the dedicated technical assistance.

References

Akinyemi, A.J., Faboya, O.L., Paul, A.A., Olayide, I., Faboya, O.A., Oluwasola, T.A., 2018. Nephroprotective effect of essential oils from ginger (zingiber officinale) and turmeric (curcuma longa) rhizomes against cadmium-induced nephrotoxicity in rats. J. Oleo Sci. 67, 1339–1345. https://doi.org/10.5650/jos.ess18115.

Andreucci, M., Faga, T., Pisani, A., Perticone, M., Michael, A., 2017. The ischemic/nephrotoxic acute kidney injury and the use of renal biomarkers in clinical practice. Eur. J. Intern. Med. 39, 1–8. https://doi.org/10.1016/j.ejim.2016.12.001.

Bao, R.K., Zheng, S.F., Wang, X.Y., 2017. Selenium protects against cadmium-induced kidney apoptosis in chickens by activating the PI3K/AKT/Bcl-2 signaling pathway. Environ. Sci. Pollut. Res. Int. 24, 20342–20353. https://doi.org/10.1007/s11356-017-9422-6.

Benvenga, S., Micali, A., Pallio, G., Vita, R., Malta, C., Puzzolo, D., Irrera, N., Squadrito, F., Altavilla, D., Minutoli, L., 2019. Effects of Myo-Inositol Alone and in Combination with Seleno-L-Methionine on Cadmium-Induced Testicular Damage in Mice. (in press) in Current Molecular Pharmacology.

Bland, S.K., Schmiedt, C.W., Clark, M.E., DeLay, J., Bienzle, D., 2017. Expression of Kidney Injury Molecule-1 in healthy and diseased feline kidney tissue. Vet. Pathol. 54, 490–510. https://doi.org/10.1177/0300985817690213.

Caprio, F., D'Eufemia, M.D., Trotta, C., Campitiello, M.R., Ianniello, R., Mele, D., Colacurci, N., 2015. Myo-inositol therapy for poor-responders during IVF: a prospective controlled observational trial. J. Ovarian Res. 8, 37. https://doi.org/10.1186/s13048-015-0167-x.

Chatterjee, P.K., 2007. Novel pharmacological approaches to the treatment of renal ischemia-reperfusion injury: a comprehensive review. Naunyn Schmiedeberg's Arch. Pharmacol. 376, 1–43. https://doi.org/10.1007/s00210-007-0183-5.

Chau, J.F., Lee, M.K., Law, J.W., Chung, S.K., Chung, S.S., 2005. Sodium/myo-inositol cotransporter-1 is essential for the development and function of the peripheral nerves. FASEB J. 19, 1887–1889. https://doi.org/10.1096/fj.05-4192fje.

Chen, Z.J., Chen, J.X., Wu, L.K., Li, B.Y., Tian, Y.F., Xian, M., Huang, Z.P., Yu, R.A., 2019. Induction of endoplasmic reticulum stress by cadmium and its regulation on Nrf2 signaling pathway in kidneys of rats. Biomed. Environ. Sci. 32, 1–10. https://doi.org/10.3967/bes2019.001.

Chunhabundit, R., 2016. Cadmium exposure and potential health risk from foods in contaminated area, Thailand. Toxicol. Res. 32, 65–72. https://doi.org/10.5487/TR.2016.32.1.065.

Condorelli, R.A., La Vignera, S., Bellanca, S., Vicari, E., Calogero, A.E., 2012. Myoinositol: does it improve sperm mitochondrial function and sperm motility? Urology 79, 1290–1295. https://doi.org/10.1016/j.urology.2012.03.005.

Condorelli, R.A., La Vignera, S., Di Bari, F., Unfer, V., Calogero, A.E., 2011. Effects of myoinositol on sperm mitochondrial function in-vitro. Eur. Rev. Med. Pharmacol. Sci. 15, 129–134.

Dai, Z., Chung, S.K., Miao, D., Lau, K.S., Chan, A.W., Kung, A.W., 2011. Sodium/myo-inositol cotransporter 1 and myo-inositol are essential for osteogenesis and bone formation. J. Bone Miner. Res. 26, 582–590. https://doi.org/10.1186/1423-0127-18-2.

Dinicola, S., Minini, M., Unfer, V., Verna, R., Cucina, A., Bizzarri, M., 2017. Nutritional and acquired deficiencies in inositol bioavailability. Correlations with metabolic disorders. Int. J. Mol. Sci. 18, 2187. https://doi.org/10.3390/ijms18102187.

Ellman, G.I., 1959. Tissue sulphydryl groups. Arch. Biochem. Biophys. 82, 70–77.

Flohé, L., Günzler, W.A., 1984. Assays of glutathione peroxidase. Methods Enzymol. 105, 114–121.

Förstermann, U., Sessa, W.C., 2012. Nitric oxide synthases: regulation and function. Eur.

Heart J. 33, 829–837. https://doi.org/10.1093/eurheartj/ehr304.
Fouad, A.A., Jresat, I., 2011. Protective effect of telmisartan against cadmium-induced nephrotoxicity in mice. Life Sci. 89, 29–35. https://doi.org/10.1016/j.lfs.2011.04.019.
Gao, P., Xu, B., Song, P., Zhu, X., Yuan, S., Kanwar, Y.S., Sun, L., 2018. The kidney specific protein myo-inositol oxygenase, a potential biomarker for diabetic nephropathy. Kidney Blood Press. Res. 43, 1772–1785. https://doi.org/10.1159/000495635.
Gobe, G., Crane, D., 2010. Mitochondria, reactive oxygen species and cadmium toxicity in the kidney. Toxicol. Lett. 198, 49–55. https://doi.org/10.1016/j.toxlet.2010.04.013.
Gong, P., Chen, F., Liu, X., Gong, X., Wang, J., Ma, Y., 2012. Protective effect of caffeic acid phenethyl ester against cadmium-induced renal damage in mice. J. Toxicol. Sci. 37, 415–425. https://doi.org/10.2131/jts.37.415.
Gu, S.Y., Yeh, T.Y., Lin, S.Y., Peng, F.C., 2016. Unfractionated bone marrow cells attenuate paraquat-induced glomerular injury and acute renal failure by modulating the inflammatory response. Sci. Rep. 6, 23287. https://doi.org/10.1038/srep23287.
Hagar, H., Al Malki, W., 2014. Betaine supplementation protects against renal injury induced by cadmium intoxication in rats: role of oxidative stress and caspase-3. Environ. Toxicol. Pharmacol. 37, 803–811. https://doi.org/10.1016/j.etap.2014.02.013.
Ichimura, T., Asseldonk, E.J., Humphreys, B.D., Gunaratnam, L., Duffield, J.S., Bonventre, J.V., 2008. Kidney injury molecule-1 is a phosphatidylserine receptor that confers a phagocytic phenotype on epithelial cells. J. Clin. Investig. 118, 1657–1668. https://doi.org/10.1172/JCI34487.
Jiang, W.D., Wu, P., Kuang, S.Y., Liu, Y., Jiang, J., Hu, K., Li, S.H., Tang, L., Feng, L., Zhou, X.Q., 2011. Myo-inositol prevents copper-induced oxidative damage and changes in antioxidant capacity in various organs and the enterocytes of juvenile jian carp (Cyprinus carpio var. Jian). Aquat. Toxicol. 105, 543–551. https://doi.org/10.1016/j.aquatox.2011.08.012.
Kim, K.S., Lim, H.J., Lim, J.S., Son, J.Y., Lee, J., Lee, B.M., Chang, S.C., Kim, H.S., 2018. Curcumin ameliorates cadmium-induced nephrotoxicity in Sprague-Dawley rats. Food Chem. Toxicol. 114, 34–40. https://doi.org/10.1016/j.fct.2018.02.007.
Kiss, E., Adams, J., Gröne, H.J., Wagner, J., 2003. Isotretinoin ameliorates renal damage in experimental acute renal allograft rejection. Transplantation 76, 480–489. https://doi.org/10.1097/01.TP.0000066354.31050.5A.
Koedrith, P., Seo, Y.R., 2011. Advances in carcinogenic metal toxicity and potential molecular markers. Int. J. Mol. Sci. 12, 9576–9595. https://doi.org/10.3390/ijms12129576.
Lee, J., Lim, K.T., 2011. Inhibitory effect of plant-originated glycoprotein (27 kDa) on expression of matrix metalloproteinase-9 in cadmium chloride-induced BNL CL.2 cells. J. Trace Elem. Med. Biol. 25, 239–246. https://doi.org/10.1016/j.jtemb.2011.08.142.
Li, S.A., Jiang, W.D., Feng, L., Liu, Y., Wu, P., Jiang, J., Kuang, S.Y., Tang, L., Tang, W.N., Zhang, Y.A., Tang, X., Shi, H.Q., Zhou, X.Q., 2017. Dietary myo-inositol deficiency decreased the growth performances and impaired intestinal physical barrier function partly relating to nrf2, jnk, e2f4 and mlck signaling in young grass carp (Ctenopharyngodon idella). Fish Shellfish Immunol. 67, 475–492. https://doi.org/10.1016/j.fsi.2017.06.032.
Li, Y., Hou, D., Chen, X., Zhu, J., Zhang, R., Sun, W., Li, P., Tian, Y., Kong, X., 2018. Hydralazine protects against renal ischemia-reperfusion injury in rats. Eur. J. Pharmacol. S0014–2999 (18), 30670–30678. https://doi.org/10.1016/j.ejphar.2018.11.015.
Liu, M., Reddy, N.M., Higbee, E.M., Potteti, H.R., Noel, S., Racusen, L., Kensler, T.W., Sporn, M.B., Reddy, S.P., Rabb, H., 2014. The Nrf2 triterpenoid activator, CDDO-imidazolide, protects kidneys from ischemia reperfusion injury in mice. Kidney Int. 85, 134–141. https://doi.org/10.1038/ki.2013.357.
Luo, T., Liu, G., Long, M., Yang, J., Song, R., Wang, Y., Yuan, Y., Bian, J., Liu, X., Gu, J., Zou, H., Liu, Z., 2017. Treatment of cadmium-induced renal oxidative damage in rats by administration of alpha-lipoic acid. Environ. Sci. Pollut. Res. Int. 24, 1832–1844. https://doi.org/10.1007/s11356-016-7953-x.
Manna, P., Sinha, M., Sil, P.C., 2009. Taurine plays a beneficial role against cadmium-induced oxidative renal dysfunction. Amino Acids 36, 417–428. https://doi.org/10.1007/s00726-008-0094-x.
Micali, A., Pallio, G., Irrera, N., Marini, H., Trichilo, V., Puzzolo, D., Pisani, A., Malta, C., Santoro, G., Laurà, R., Santoro, D., Squadrito, F., Altavilla, D., Germanà, A., Minutoli, L., 2018. Flavocoxid, a natural antioxidant, protects mouse kidney from cadmium-induced toxicity. Oxidative Med. Cell. Longev. 2018, 9162946. https://doi.org/10.1155/2018/9162946.
Min, K.S., Kim, H., Fujii, M., Tetsuchikawahara, N., Onosaka, S., 2002. Glucocorticoids suppress the inflammation-mediated tolerance to acute toxicity of cadmium in mice. Toxicol. Appl. Pharmacol. 178, 1–7. https://doi.org/10.1006/taap.2001.9323.
Minutoli, L., Micali, A., Pisani, A., Puzzolo, D., Bitto, A., Rinaldi, M., Pizzino, G., Irrera, N., Galfo, F., Arena, S., Pallio, G., Mecchio, A., Germanà, A., Bruschetta, D., Laurà, R., Magno, C., Marini, H., Squadrito, F., Altavilla, D., 2015. Flavocoxid protects against cadmium-induced disruption of the blood–testis barrier and improves testicular damage and germ cell impairment in mice. Toxicol. Sci. 148, 311–329. https://doi.org/10.1093/toxsci/kfv185.
Mohajeri, M., Rezaee, M., Sahebkar, A., 2017. Cadmium-induced toxicity is rescued by curcumin: a review. Biofactors 43, 645–661. https://doi.org/10.1002/biof.1376.
Morales, A.I., Vicente-Sánchez, C., Sandoval, J.M., Egido, J., Mayoral, P., Arévalo, M.A., Fernández-Tagarro, M., López-Novoa, J.M., Pérez-Barriocanal, F., 2006. Protective effect of quercetin on experimental chronic cadmium nephrotoxicity in rats is based on its antioxidant properties. Food Chem. Toxicol. 44, 2092–2100 doi.org/10.1016/j.fct.2006.07.012.
Moulis, J.M., Thévenod, F., 2010. New perspectives in cadmium toxicity: an introduction. Biometals 23, 763–768. https://doi.org/10.1007/s10534-010-9365-6.
Muscogiuri, G., Palomba, S., Laganà, A.S., Orio, F., 2016. Inositols in the treatment of insulin-mediated diseases. Internet J. Endocrinol. 2016, 3058393. https://doi.org/10.1155/2016/3058393. Epub 2016 Sep 8. Review. Erratum in: Int J Endocrinol. 2016;2016:6189820. doi: 10.1155/2016/6189820.
Nayak, B., Kondeti, V.K., Xie, P., Lin, S., Viswakarma, N., Raparia, K., Kanwar, Y.S., 2011. Transcriptional and post-translational modulation of myo-inositol oxygenase by high glucose and related pathobiological stresses. J. Biol. Chem. 286, 27594–27611. https://doi.org/10.1074/jbc.M110.217141.
Nazima, B., Manoharan, V., Miltonprabu, S., 2015. Grape seed proanthocyanidins ameliorates cadmium-induced renal injury and oxidative stress in experimental rats through the up-regulation of nuclear related factor 2 and antioxidant responsive elements. Biochem. Cell Biol. 93, 210–226. https://doi.org/10.1139/bcb-2014-0114.
Okada, H., Senmaru, T., Fukui, M., Kondo, Y., Ishigami, A., Maruyama, N., Obayashi, H., Yamazaki, M., Nakamura, N., Hasegawa, G., 2015. Senescence marker protein-30/gluconolactonase deficiency exacerbates diabetic nephropathy through tubular injury in a mouse model of type 1 diabetes. J. Diabetes Invest. 6, 35–43. https://doi.org/10.1111/jdi.12252.
Park, J.H., Choi, J.W., Ju, E.J., Pae, A.N., Park, K.D., 2015. Antioxidant and anti-inflammatory activities of a natural compound, shizukahenriol, through Nrf2 activation. Molecules 20, 15989–16003. https://doi.org/10.3390/molecules200915989.
Pintaudi, B., Di Vieste, G., Bonomo, M., 2016. The effectiveness of myo-inositol and D-chiro inositol treatment in type 2 diabetes. Internet J. Endocrinol. 2016, 9132052. https://doi.org/10.1155/2016/9132052.
Prozialeck, W.C., Edwards, J.R., Lamar, P.C., Liu, J., Vaidya, V.S., Bonventre, J.V., 2009. Expression of kidney injury molecule-1 (Kim-1) in relation to necrosis and apoptosis during the early stages of Cd-induced proximal tubule injury. Toxicol. Appl. Pharmacol. 238, 306–314. https://doi.org/10.1016/j.taap.2009.01.016.
Prozialeck, W.C., Edwards, J.R., 2012. Mechanisms of cadmium-induced proximal tubule injury: new insights with implications for biomonitoring and therapeutic interventions. J. Pharmacol. Exp. Ther. 343, 2–12. https://doi.org/10.1124/jpet.110.166769.
Prozialeck, W.C., Vaidya, V.S., Liu, J., Waalkes, M.P., Edwards, J.R., Lamar, P.C., Bernard, A.M., Dumont, X., Bonventre, J.V., 2007. Kidney injury molecule-1 is an early biomarker of cadmium nephrotoxicity. Kidney Int. 72, 985–993. https://doi.org/10.1038/sj.ki.5002467.
Rafati, A., Hoseini, L., Babai, A., Noorafshan, A., Haghbin, H., Karbalay-Doust, S., 2015. Mitigating effect of resveratrol on the structural changes of mice liver and kidney induced by cadmium; a stereological study. Prev. Nutr. Food Sci. 20, 266–275. https://doi.org/10.3746/pnf.2015.20.4.266.
Ramesh, G., Reeves, W.B., 2002. TNF-alpha mediates chemokine and cytokine expression and renal injury in cisplatin nephrotoxicity. J. Clin. Investig. 110, 835–842. https://doi.org/10.1172/JCI15606.
Rani, A., Kumar, A., Lal, A., Pant, M., 2014. Cellular mechanisms of cadmium-induced toxicity: a review. Int. J. Environ. Health Res. 24, 378–399. https://doi.org/10.1080/09603123.2013.835032.
Sun, L., Dutta, R.K., Xie, P., Kanwar, Y.S., 2016. Myo-inositol oxygenase overexpression accentuates generation of reactive oxygen species and exacerbates cellular injury following high glucose ambience: a new mechanism relevant to the pathogenesis of diabetic nephropathy. J. Biol. Chem. 291, 5688–5707. https://doi.org/10.1074/jbc.M115.669952.
Thévenod, F., Lee, W.K., 2013. Toxicology of cadmium and its damage in mammalian organs. In: Sigel, A., Sigel, H., Sigel, R.K.O. (Eds.), Cadmium, from Toxicity to Essentiality. Met Ions Life Sci, vol 11. pp. 415–490. https://doi.org/10.1007/978-94-007-5179-8_14.
Thévenod, F., 2009. Cadmium and cellular signaling cascades: to be or not to be? Toxicol. Appl. Pharmacol. 238, 221–239. https://doi.org/10.1016/j.taap.2009.01.013.
Thévenod, F., 2003. Nephrotoxicity and the proximal tubule. Insights from cadmium. Nephron. Physiol. 93, 87–93 doi.org/10.1159/000070241.
Tinkov, A.A., Filippini, T., Ajsuvakova, O.P., Aaseth, J., Gluhcheva, Y.G., Ivanova, J.M., Bjørklund, G., Skalnaya, M.G., Gatiatulina, E.R., Popova, E.V., Nemereshina, O.N., Vinceti, M., Skalny, A.V., 2017. The role of cadmium in obesity and diabetes. Sci. Total Environ. 601–602, 741–755. https://doi.org/10.1016/j.scitotenv.2017.05.224.
Tsutsumi, T., Ishihara, A., Yamamoto, A., Asaji, H., Yamakawa, S., Tokumura, A., 2014. The potential protective role of lysophospholipid mediators in nephrotoxicity induced by chronically exposed cadmium. Food Chem. Toxicol. 65, 52–62. https://doi.org/10.1016/j.fct.2013.12.019.
Wang, M., Liu, R., Jia, X., Mu, S., Xie, R., 2010. N-acetyl-seryl-aspartyl-lysyl-proline attenuates renal inflammation and tubulointerstitial fibrosis in rats. Int. J. Mol. Med. 26, 795–801. https://doi.org/10.3892/ijmm_00000527.
Wise, J.T.F., Wang, L., Zhang, Z., Shi, X., 2017. The 9th conference on metal toxicity and carcinogenesis: the conference overview. Toxicol. Appl. Pharmacol. 331, 1–5. https://doi.org/10.1016/j.taap.2017.04.007.
Yamamoto, Y., Maeshima, Y., Kitayama, H., Kitamura, S., Takazawa, Y., Sugiyama, H., Yamasaki, Y., Makino, H., 2004. Tumstatin peptide, an inhibitor of angiogenesis, prevents glomerular hypertrophy in the early stage of diabetic nephropathy. Diabetes 53, 1831–1840. https://doi.org/10.2337/diabetes.53.7.1831.
Yang, H., Shu, Y., 2015. Cadmium transporters in the kidney and cadmium-induced nephrotoxicity. Int. J. Mol. Sci. 16, 1484–1494. https://doi.org/10.3390/ijms16011484.
Yang, T., Vesey, D.A., Johnson, D.W., Wei, M.Q., Gobe, G.C., 2007. Apoptosis of tubulointerstitial chronic inflammatory cells in progressive renal fibrosis after cancer therapies. Transl. Res. 150, 40–50. https://doi.org/10.1016/j.trsl.2007.01.006.